Corrections for Horizontal Winds and Wind Shear in Raindrop Size Spectrometers

J. G. HOSKING,* C. D. STOW AND S. G. BRADLEY

Department of Physics, The University of Auckland, Auckland, New Zealand

(Manuscript received 2 April 1984, in final form 3 December 1984)

ABSTRACT

The effect of horizontal drag forces on raindrop trajectories is shown to influence strongly the detection efficiencies computed for drop cameras and disdrometers. Two examples of sheared flow involving real instruments are studied and it is found that whereas detection efficiencies remain high for both large and small drops, low detection efficiencies occur for drops of radius near 0.2 mm. These predictions are tested against field results from one of the instruments and it is shown that the theory of Rinehart is inadequate for small drops for this instrument.

1. Introduction

The measurement of the size spectra of raindrops and related cumulative quantities such as rainfall rate is of great importance to meteorologists. It is therefore important to examine sources of error that are likely to bias such measurements. One possible source of error is due to wind. Sevruk (1982), for instance, has studied catch loss in raingages due to wind deformation above the gage orifice. Griffiths (1975), Bradley and Stow (1975), Stow and Jones (1981) and Rinehart (1983) have examined the effect of bias due to tilting of instruments in the presence of wind. Rinehart (1983) has also examined the effect of wind on measurements of drop size spectra made using a drop camera. His calculations indicated that a horizontal wind component caused a bias of a measured drop size spectrum sufficient to convert an incident exponential drop size spectrum into a lognormal-like one. His calculations, however, neglect the effect of horizontal drag on the drops if they enter a stagnant airspace inside the drop camera. A theory which includes a correction for this horizontal drag is developed below.

2. Theory

The equation of motion of a drop of mass m falling with velocity $\mathbf{V}$ is given by

$$m\frac{d\mathbf{V}}{dt} = m\mathbf{g}' - \mathbf{F}_D \qquad (1)$$

where $\mathbf{F}_D$ is the drag force and $\mathbf{g}'$ is the downward acceleration of gravity corrected for buoyancy. Eq. (1) may be rewritten as

$$m\frac{d\mathbf{V}}{dt} = m\mathbf{g}' - 6\pi r\eta(\mathbf{V} - \mathbf{W})\frac{C_D N_{\mathrm{Re}}}{24} \qquad (2)$$

where N_{Re} is the Reynolds number $2r\rho V'/\eta$, C_D is the drag coefficient $2F_D/\pi r^2\rho V'^2$, $\mathbf{W}$ is the velocity of the air, and $V' = |\mathbf{V} - \mathbf{W}|$; r is the radius of a sphere of volume equal to that of the drop; ρ and η are the density and dynamic viscosity of the air.

In order to solve Eq. (2) the instantaneous drag coefficient must be known for an accelerating drop; this will be a function of both N_{Re} and the drop shape. Wang and Pruppacher (1977) have solved Eq. (2) for the one-dimensional vertical motion case. They assumed that the instantaneous drag coefficient required was identical to that of a drop of different size falling at terminal velocity with the same Reynolds number. In this way Wang and Pruppacher produced trajectories for drops starting from rest that were in good agreement with experiment. Beard (1977b) has also confirmed the applicability of these approximations. Following this approach, use is made of the formulae of Berry and Pranger (1974) relating C_D to N_{Re}; effects due to drop oscillation are ignored. Two vertical profiles for the horizontal wind near the ground are used in the treatment which follows.

Consider a drop initially falling at terminal velocity $\mathbf{V}_T$ through a region with wind profile $\mathbf{W}$ (the terminal velocity may be calculated using the ninth-order polynomial fit of Beard, 1977a). If the vertical component of the wind is assumed to be negligible, Eq. (2) may be resolved into the following orthogonal components

$$m\frac{dV_x}{dt} = -6\pi r\eta(V_x - W_x)\left(\frac{C_D N_{\mathrm{Re}}}{24}\right), \qquad (3a)$$

$$m\frac{dV_z}{dt} = mg' - 6\pi r\eta V_z\left(\frac{C_D N_{\mathrm{Re}}}{24}\right). \qquad (3b)$$

where z is directed upward and x horizontally. Spec-

* Current affiliation: Department of Computer Science, University of Auckland, Auckland, New Zealand.

ification of the wind profile $W_x(z)$ then enables the Equations (3a) and (3b) to be solved using a Runge–Kutta method. Particular attention has been given to the recalculation of instrument catch efficiency under the condition $W_x(z)$ = constant outside the instrument and $W_x(z) = 0$ within the instrument.

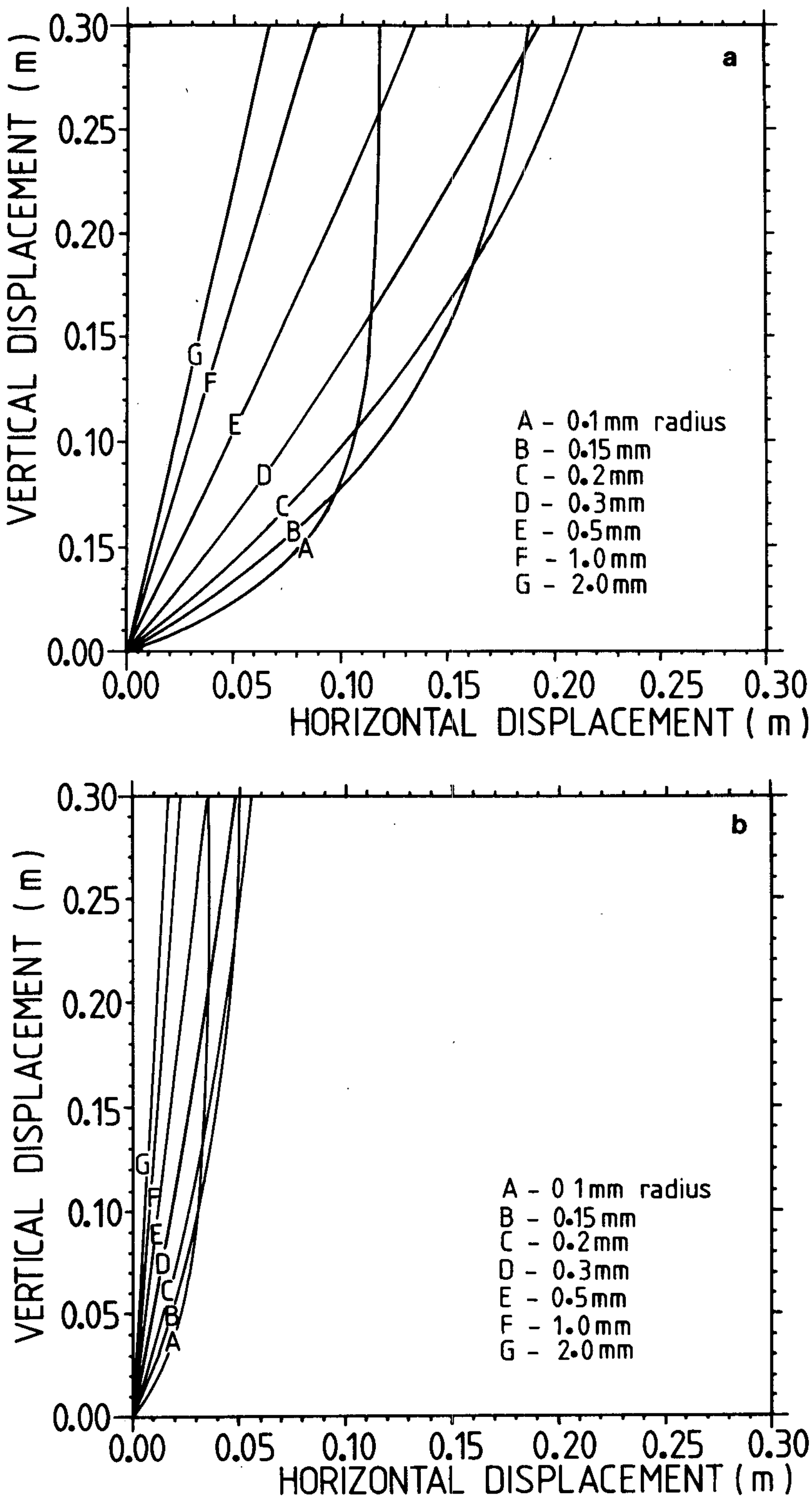

FIG. 1. Trajectories of raindrops falling into stagnant air as a function of drop radius and external horizontal windspeed W_x; (a) $W_x = 2$ m s^{-1}, (b) $W_x = 0.5$ m s^{-1}.

The effect of using a more realistic wind profile of the form proposed by Sutton (1949) in which

$$W_x(z) = W_x(z_0)\left(\frac{z}{z_0}\right)^m, \qquad (4)$$

where z_0 is a reference level and m is a constant dependent upon ground roughness and the stability of the air, is also considered below.

3. Results and discussion

a. Theoretical

Figure 1 shows drop trajectories calculated using Eqs. (3a) and (3b) for several drop radii values in horizontal winds of either 0.5 or 2 m s^{-1}. As expected, smaller drops decelerate more quickly than larger ones, and the drop size at which maximum horizontal deflections occurs increases with fall height. This is in contrast to the trajectories of Rinehart which appear as straight lines that at the origin are tangential to the curves in Fig. 1.

Equation (3a) and (3b) imply a coupling between the horizontal and vertical motion of a drop and it is to be expected that drops entering the stagnant volume will suffer a temporary decrease in their fall speed whilst horizontal accelerations exist. This effect is demonstrated in Table 1, which shows peak fall-speed reductions for drops initially falling at terminal velocity, and the time and fall-height required to reach them, for a range of drop sizes and horizontal winds. Departures from terminal velocity are significant for the smaller drops even for light winds. Large drops require much longer times to reach their minimum fall speed than do small ones.

TABLE 1. Maximum fall speed reductions ΔV from still-air terminal velocity for drops of different sizes and different initial horizontal velocities falling into a stagnant airspace. The time t and fall distance Δz taken by drops to reach max ΔV are also shown.

r (mm)	max ΔV (%)	t (s)	Δz (m)
	$W_x = 5$ m s^{-1}		
0.1	27.0	0.051	0.028
0.2	16.0	0.110	0.15
0.5	6.6	0.215	0.82
1.0	4.5	0.335	2.12
2.0	4.2	0.464	3.98
	$W_x = 10$ m s^{-1}		
0.1	38	0.049	0.024
0.2	28	0.104	0.13
0.5	18	0.216	0.75
1.0	14	0.317	1.87
2.0	12	0.401	3.24
	$W_x = 20$ m s^{-1}		
0.1	48	0.043	0.019
0.2	41	0.091	0.099
0.5	34	0.191	0.57
1.0	30	0.278	1.40
2.0	28	0.335	2.33

The new trajectories (of Fig. 1) may be used to evaluate a possible bias in the determination of drop size spectra obtained by the Illinois State Water Survey (ISWS) raindrop camera (Jones, 1959; Rinehart, 1983). Unlike many other drop spectrometers, the geometry of the ISWS camera does not necessarily require the air in the sample volume to be stagnant. However, for the purpose of comparing our model with the previous treatment of Rinehart, a stagnant airspace is assumed. Following Rinehart, the wind is assumed to be blowing across the rectangular opening in the camera. The proportion of the sample volume accessible to any given size of drop may be calculated if the wind speed is known; this proportion is called the relative sample volume. Corrections to the calculation of the relative sample volume to include variations in vertical fall speed of the drops show that the detection efficiency of small drops is slightly increased but the correction is negligible.

Figure 2 shows the relative sample volume of the drop camera as a function of windspeed and drop radius using the present theory, and in comparison Fig. 3 shows those previously determined by Rinehart. The significant differences between the two treatments appear for drops smaller than about 0.5 mm radius and may be reexpressed by examining the modification of an incident exponential drop size spectrum caused by sampling with the drop camera; this is shown in Fig. 4. It may be seen that the present theory predicts little bias for the very small drops while the lognormal distributions generated by Rinehart's calculations predict a severe depletion in the same drop size region.

There now follows a similar examination of the bias introduced by wind during the use of the optical disdrometer described by Stow and Jones (1981); this device is currently being used in field measurements by us. Raindrops enter through a circular aperture 40 cm above the ground and fall 15 cm before encountering the first sample volume; a second sample volume is situated 9 cm below the first. Drops are timed during their fall and those whose trajectories do not pass through the second detector may be identified; occupation of the volume between the two detectors by more than one drop may also be monitored. Figure 5 shows calculated detection efficiencies for the first sample volume as a function of windspeed and drop radius. The efficiencies are qualitatively similar to those of the drop camera showing a minimum in the region of drop radius between 0.15 and 0.25 mm. The disdrometer is much more seriously affected by moderate to high winds than the ISWS instrument because of the small ratio of aperture size to internal fall depth. For light winds, the disdrometer performs somewhat better than the ISWS camera for

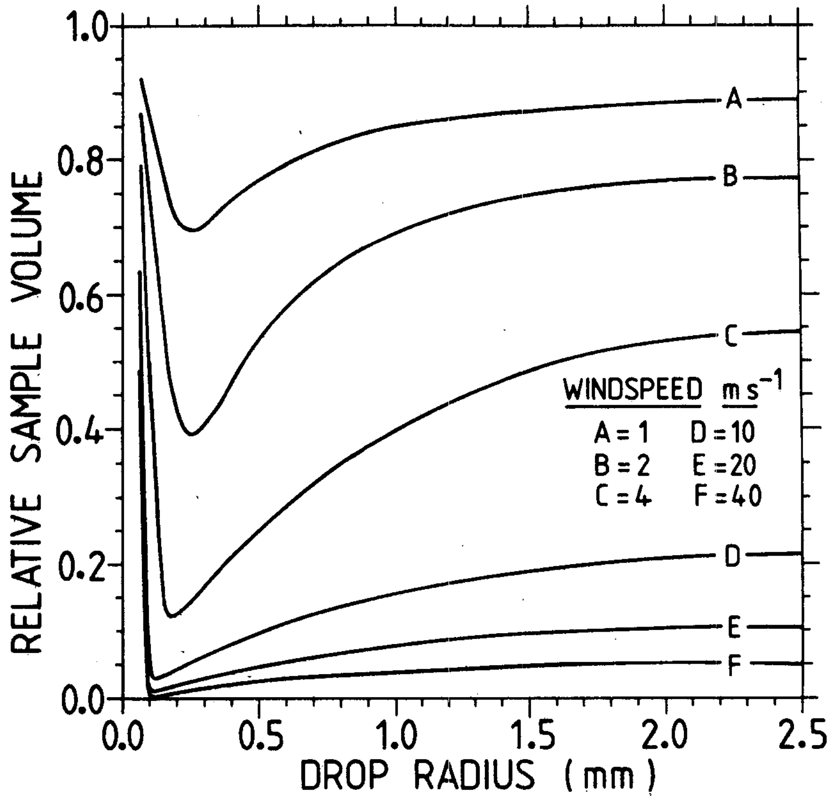

FIG. 2. Relative sample volume versus drop radius for a range of horizontal wind speeds using the camera described by Rinehart (1983). Worst-case situation, i.e., when the wind blows along the length of the camera.

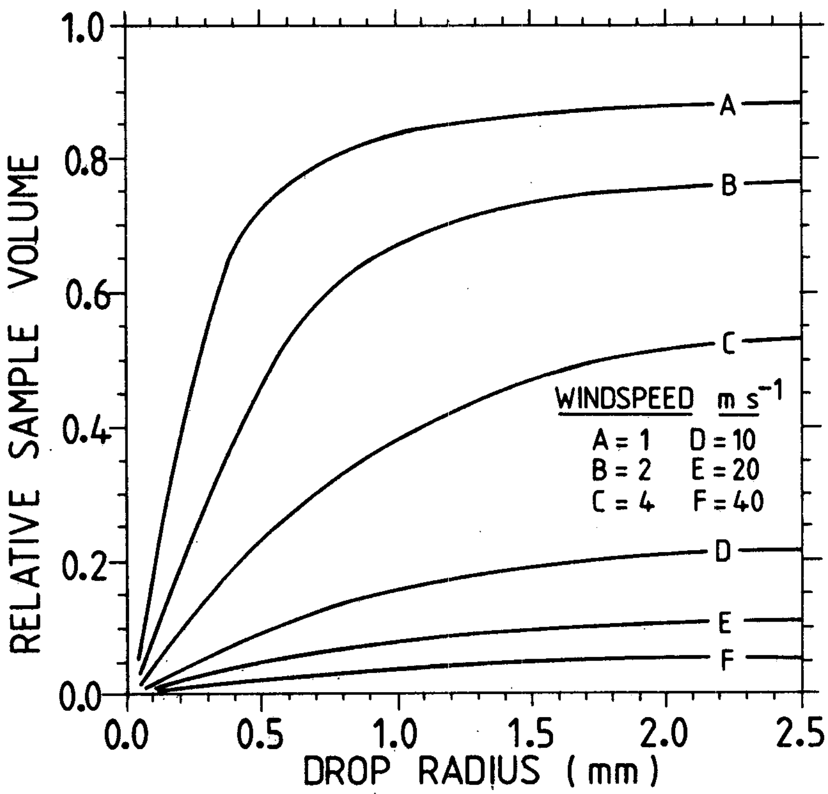

FIG. 3. As in Fig. 2, but using the treatment of Rinehart.

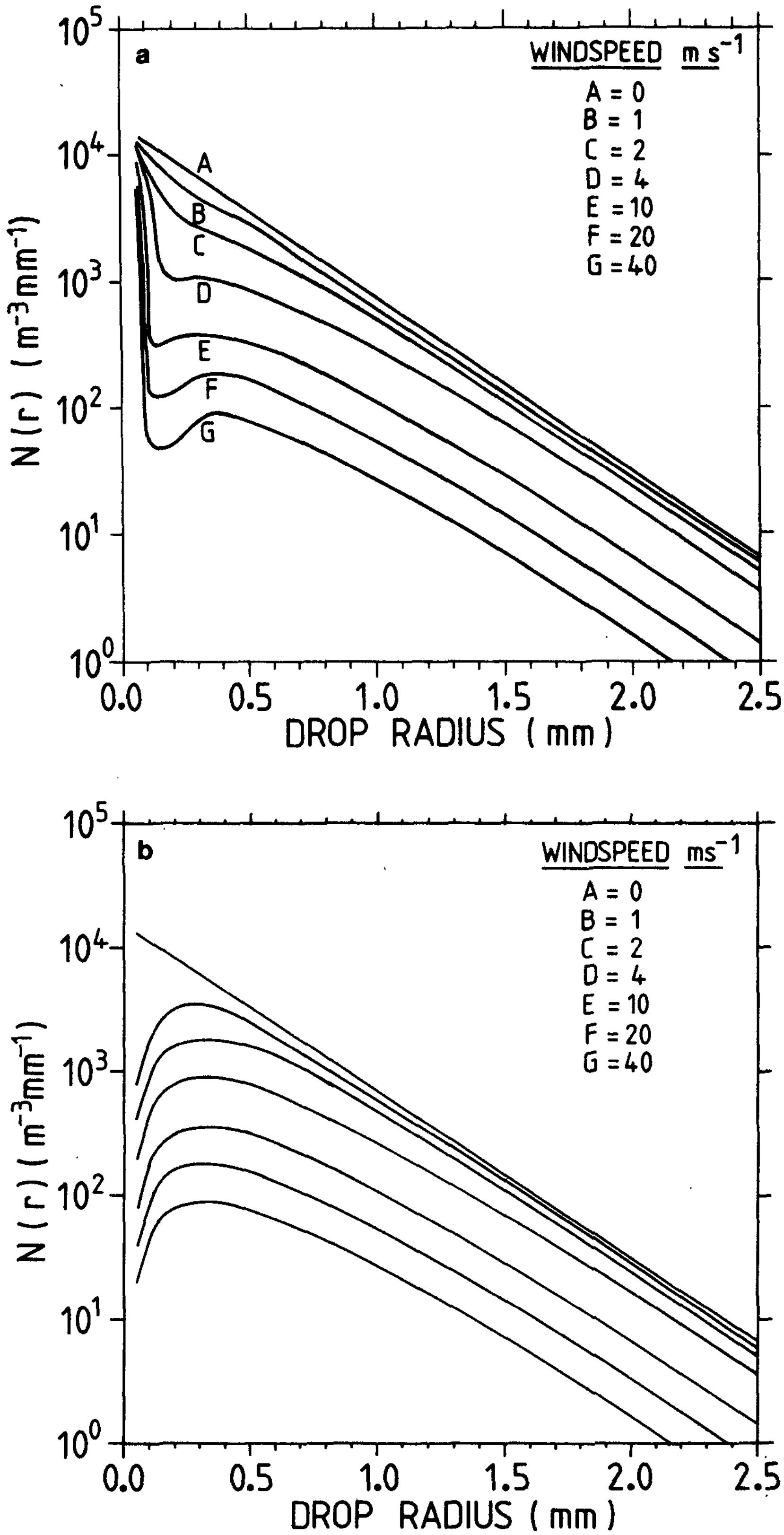

FIG. 4. The effects of windspeed on an initial exponential drop size distribution sampled by the raindrop camera. The distribution is Marshall–Palmer (1948) for a rainrate of 100 mm h^{-1}. (a) Using the present theory, (b) according to Rinehart.

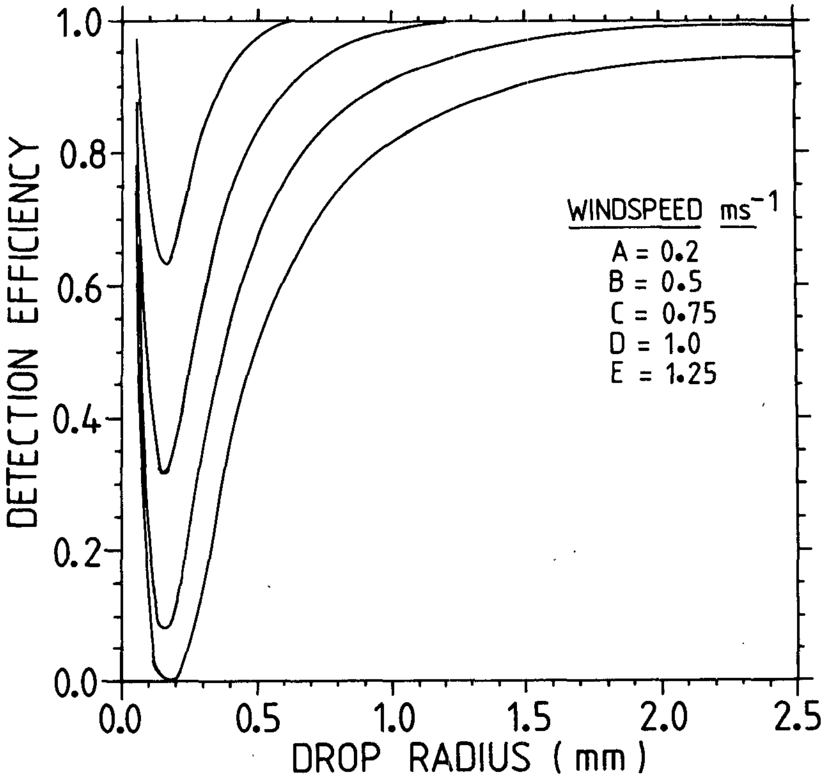

FIG. 5. Detection efficiency as a function of windspeed and drop radius for the optical disdrometer of Stow and Jones (1981) (top detector only).

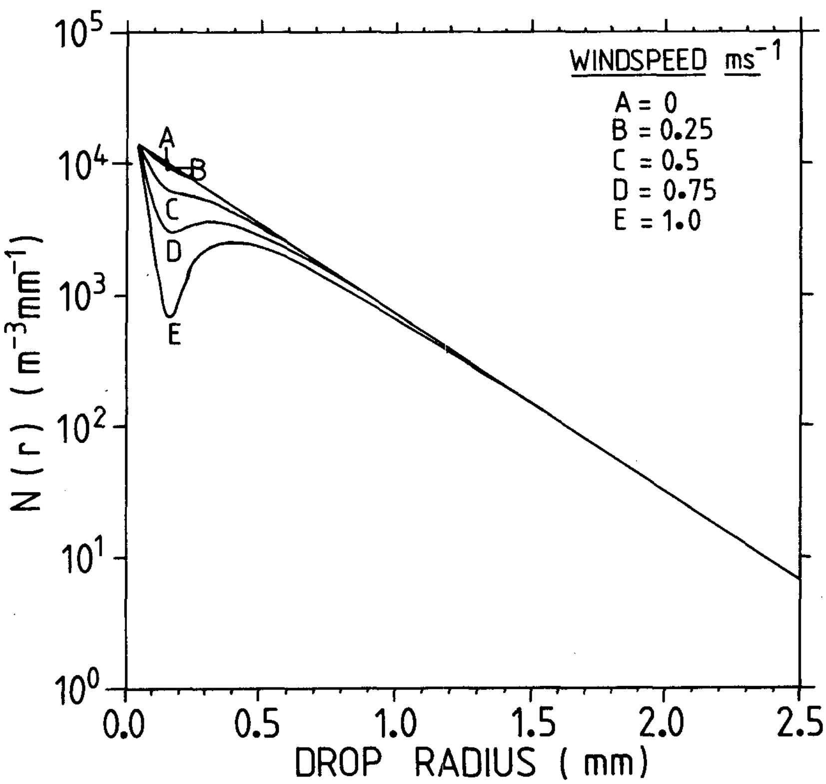

FIG. 6. The effects of windspeed on an exponential distribution sampled by the optical disdrometer; the initial distribution is as in Fig. 5.

drops of radius greater than about 0.7 mm radius. The corresponding modification of an incident exponential size distribution is shown in Fig. 6.

In all of the above calculations it has been assumed that drops have a horizontal velocity component equal to the wind speed when they enter the region of stagnation within the instrument. In the presence of the usual wind shear near the ground, this assumption is unlikely to be true, and it is desirable to investigate what further spectral corrections may be necessary on this account. Using the profile of Eq. (4), Fig. 7 shows the corresponding drop-velocity profiles obtained using Eqs. (3a) and (3b) with $z_0 = 10$ m, $V_w(0) = 10$ m s^{-1}, and $m = 0.25$. While the smaller drops follow the wind profile closely, the larger drops do not. Thus the larger drops enter apertures near the ground at angles closer to the horizontal than those used above to calculate detection efficiencies and relative sample volumes.

The overall effect of the correction for any profile qualitatively similar to that represented by Eq. (4) is to decrease the detection efficiency and relative sample volume for large drops whilst those for smaller drops remain essentially unaltered when compared with the no-wind situation. The vertical velocities of drops show a decrease from terminal velocity as they approach the ground in a manner similar to that when entering stagnant air. However, here the velocity changes are small, though larger for the bigger drops; for these the velocity change is less than 5% when $W(z_0) = 10$ m s^{-1}. Momentum-type disdrometers such as that of Joss and Waldvogel (1967) therefore appear to require no correction for this effect.

b. Experimental evidence

The present authors have been operating the dual-beam disdrometer described by Stow and Jones (1981) for many months in the field. The wind corrections described in this paper require that the upper and lower raindrop detectors have relative collection efficiencies which vary with wind speed in a calculable way, which can be compared with experimental data. In the disdrometer the lack of appearance of a drop in the lower detector previously measured at the upper detector generates a "time out" error signal which is recorded; the "time out" data therefore link the collection efficiencies of the two size detectors. To a close approximation, for any given narrow range of drop sizes, the ratio R of the collection efficiency of the lower drop detector to that of the upper one is given by

$$R = \frac{\text{drop count in upper detector} - \text{"time out" count}}{\text{drop count in upper detector}}.$$

Data were collected over a four-hour period during

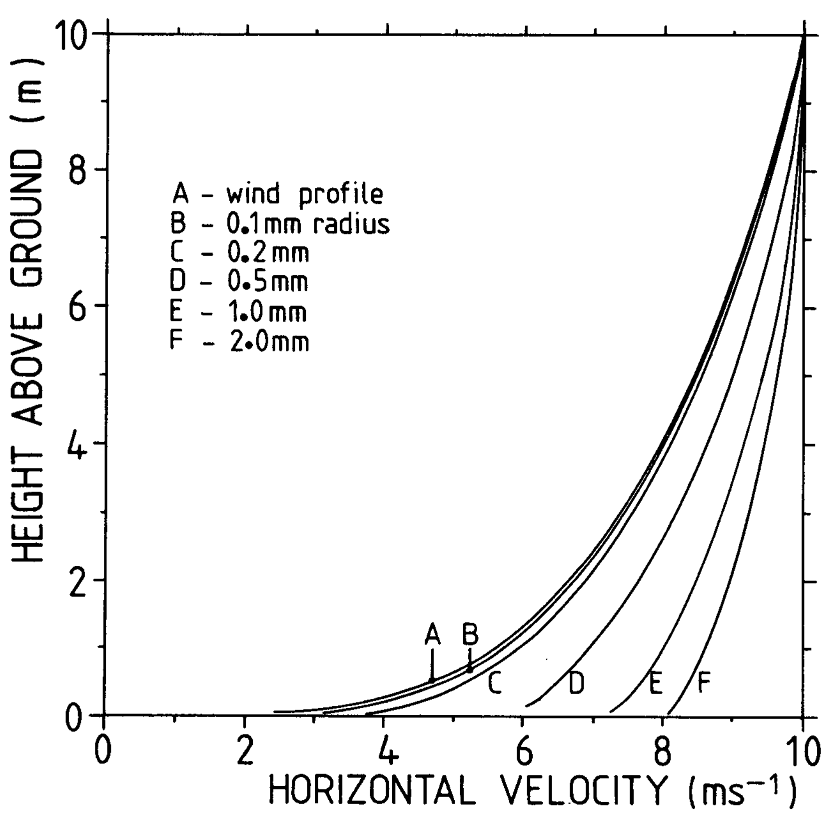

FIG. 7. Horizontal velocity profiles for drops falling from 10 m through a region of windshear. The windspeed at 10 m is 10 m s^{-1}.

frontal rain on 30 July 1983. Wind speeds were measured 6 m above the ground and can be used via Eq. (4) to estimate the wind speed at the disdrometer aperture; it has been assumed that the required value of the parameter m lies in the range $m = 0.25$–0.50. Because the greatest difference between the present theory and Rinehart's is apparent for very small drops, it was decided to determine R using drops in the radius range 0.15 ± 0.05 mm. For such small drops the horizontal speed at the entrance aperture to the disdrometer may be assumed equal to the estimated local wind. The data collection period was divided into fifteen periods of 1000 s duration and actual winds were averaged over each period. The results of the measurements and calculations are shown in Fig. 8, where it may be seen that nearly all of the experimental data points lie within the range predicted by the present theory and that none lie within the range predicted by Rinehart. Indeed, impossibly large values of m would be required to offer any reconciliation of the latters' theory with experiment.

4. Conclusions

The wind sorting of raindrops appears to be a major source of error for many types of drop spectrometers where the detection region is within a stagnant air space. In both of the devices studied, where drops are assumed to be moving at the horizontal wind speed on entry into the collecting aperture, the major effect is a reduction in detection efficiency in the 0.2 mm drop radius region. The detection efficiency for smaller drops remains high because of the deceleration of the drops due to drag, while for larger drops the efficiency remains high due to the larger terminal velocities. Experimental evidence obtained using the optical disdrometer of Stow and Jones (1981) shows the importance of considering drag forces within the instrument when there are horizontal winds present outside; in contrast to the theory described here, the simpler theoretical treatment of Rinehart (1983) is unable to predict the observed detection efficiency for small drops.

The coupling of the horizontal and vertical drop motion causes appreciable reduction of the fall speed of a drop entering into a stagnant airspace. However, this reduction has only a small effect on the detection efficiencies otherwise computed for a drop camera of the design studied.

Windshear in the atmosphere above instruments with enclosed detection volumes will also cause a

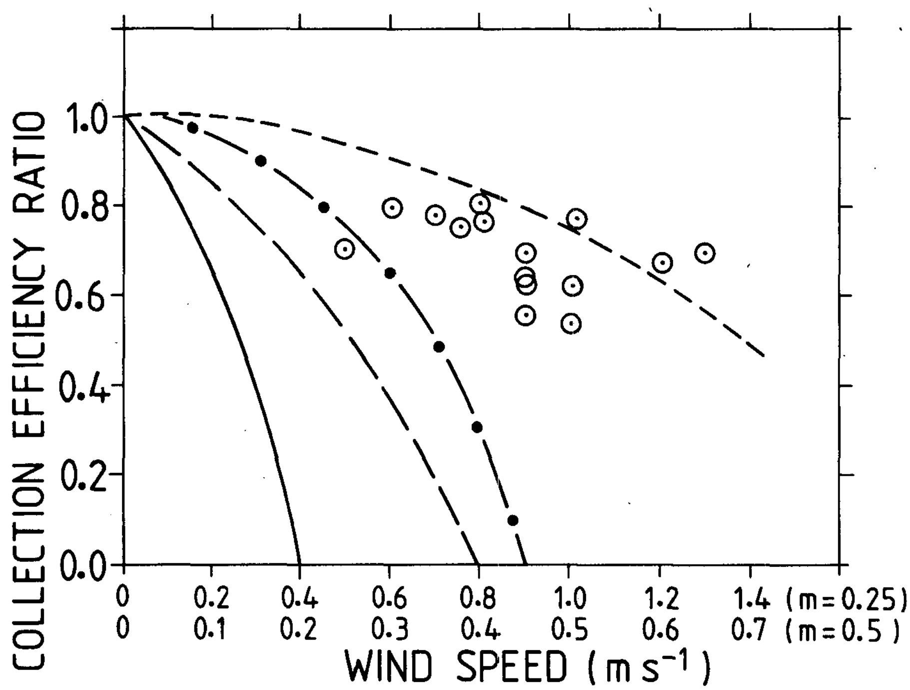

FIG. 8. The ratio of the collection efficiencies of the lower and upper detectors of the disdrometer of Stow and Jones (1981) versus horizontal windspeed at the ground [estimated from 6 m winds using Eq. (4)] for drops of radius 0.15 mm ± 0.05 mm. Dotted circles indicate experimental data points; short dashes present theory for $m = 0.5$; dash-dots present theory for $m = 0.25$; long dashes according to the theory of Rinehart (1983) for a wind profile having $m = 0.5$; and solid line according to the theory of Rinehart (1983) for a wind profile having $m = 0.25$.

bias in drop size measurement. The larger drops cannot follow the horizontal wind profile and possess a horizontal velocity in excess of the wind near ground level. Thus the larger drops enter apertures at angles closer to the horizontal than the local wind suggests; this effect reduces the detection efficiency of these drops. The simpler corrections employed by Rinehart (1983) may nevertheless be used without gross error for drops larger than about 0.5 mm in radius but they are seriously in error for the smaller drops.

The errors discussed here may be compared with the effects of rain splashing on the disdrometer and wind deformation caused by the instrument. Stow and Jones (1981) have calculated the effects of splashing at the entrance rim of their disdrometer (see their Fig. 5); the error due to such splashing is minimal. Further work is required to estimate the effects of wind flow modification, for example by extending the analysis of Sevruk (1982) to include drop size dependence.

In order to reduce biasing effects due to wind, instruments should be designed with large ratios of aperture size to internal fall depth unless the ambient wind profile can be maintained within the sample volume. Data from instruments which cannot satisfy either one or the other of these features will require correction for wind.

REFERENCES

Beard, K. V., 1977a: Terminal velocity adjustment for cloud and precipitation drops aloft. *J. Atmos. Sci.*, **34**, 1293–1298.

——, 1977b: On the acceleration of large water drops to terminal velocity. *J. Appl. Meteor.*, **16**, 1068–1071.

Berry, E. X., and M. R. Pranger, 1974: Equations for calculating the terminal velocities of water drops. *J. Appl. Meteor.*, **13**, 108–113.

Bradley, S. G., and C. D. Stow, 1975: Reply to comments on "The measurement of size and charge on raindrops," Parts I and II. *J. Appl. Meteor.*, **14**, 426–428.

Griffiths, R. F., 1975: Comments on "The measurement of size and charge on raindrops," Parts I and II, *J. Appl. Meteor.*, **14**, 422–425.

Jones, D. M. A., 1959: The shape of raindrops. *J. Meteor.*, **16**, 504–510.

Joss, V. J., and A. Waldvogel, 1967: Ein Spektrograph für niederschlastropfen mit automatischer Auswertung. *Pure Appl. Geophys.*, **68**, 240–246.

Marshall, J. S., and W. McK. Palmer, 1948: The distribution of raindrops with size. *J. Meteor.*, **5**, 165–166.

Rinehart, R. E., 1983: Out-of-level instruments: Errors in hydrometeor spectra and precipitation measurements. *J. Climate Appl. Meteor.*, **22**, 1404–1410.

Sevruk, B., 1982: Methods of correction for systematic error in point precipitation measurement for operational use. Operational Hydrology Rep. 21, WMO, 91 pp.

Stow, C. D., and K. Jones, 1981: A self evaluating disdrometer for the measurement of raindrop size and charge at the ground. *J. Appl. Meteor.*, **20**, 1160–1176.

Sutton, O. G., 1949: *Atmospheric turbulence.* Methuen, 107 pp.

Wang, P. K., and H. R. Pruppacher, 1977: Acceleration to terminal velocity of cloud and raindrops. *J. Appl. Meteor.*, **16**, 275–280.